Reducing the warp of sheet glass

Mireille Akilian
Mark L. Schattenburg

Abstract — Many leading technologies, such as flat-panel displays and precision optics, require sheet glass with exceptional surface qualities. Commercially available sheet glass of <1-mm thickness typically has a surface warp on the order of hundreds of microns, rendering it a challenge to utilize progressively thinner sheets. A novel method of shaping individual sheets and ribbons of glass is presented which utilizes porous mandrels. This method reduces the surface warp of the ribbon while in its hot state without contacting its surface. Sheet glass is inserted between two parallel porous mandrels spaced apart by a predefined distance. A thin layer of pressurized gas flows through each mandrel and out against the glass surfaces. The local gap between the warped glass sheet and the flat mandrel determines the local pressure on the glass. When in its heated and soft state, the glass sheet's surface is changed by this pressure with a strong restorative force proportional to the inverse of the gap cubed, which tends to flatten the sheet. By using flat mandrels and controlled pressurized gas at elevated temperatures, the outcome is a sheet of glass with a surface warp of a few microns while retaining its original pristine optical surface qualities.

Keywords — *Sheet glass, flat-panel displays, liquid-crystal displays, precision optics, porous bearings, flat mandrels, surface morphology.*

DOI # 10.1889/JSID18.3.240

Reprint from the Journal of the SID

1 Introduction

High-precision sheet glass is used in many applications, such as filters, touch panels, sensors, masks in the semiconductor industry, hard-disk-drive platens, cellular-phone and computer panels, flat-panel displays, and precision substrates in optical instruments, such as telescopes. In 2005, about 17.5 million flat-panel televisions were sold, generating $25.6 billion in retail revenues and making this industry the biggest market for flat glass.[1] Current screen-manufacturing technology utilizes glass sheets ranging between 0.7 and 1.1 mm thickness, depending on the size of the display, with smaller mobile devices such as personal laptops and phones utilizing glass sheets ≤0.5 mm in thickness.[2] It is desired to decrease sheet thickness to reduce the overall weight of flat-screen displays; however, one of the limiting factors in achieving this goal is the surface warp of sheets as they are currently manufactured. This warp increases with smaller sheet thicknesses and becomes more critical as the sizes of flat screens increase. Two critical parameters defined by the liquid-crystal display (LCD) industry to determine the quality of glass substrates used in displays[2,3] are:

1. Surface waviness, which represents surface errors over a length-scale of a few millimeters (between 2 and 20 mm). The maximum tolerated waviness is between 0.05 and 0.1 μm.

2. Surface warp, which represents the global surface error. The warp tolerance is <100–200 μm, depending on the size of the display.

Exceeding these parameters causes changes in the electrical response of the cells, resulting in optical irregularities including differences in gray scale. It also leads to misalignment between deposition layers, since larger surface warp reduces the ability of the stepper lens to focus correctly on the substrate during the photolithography process. Although at the current stage, a warp of 100 μm over the entire surface of a glass substrate can be tolerated, having less warp would enhance the performance of the flat-panel displays by providing a higher contrast and increasing yield because such substrates are less prone to optical errors during the flat-panel manufacturing process.

Glass used in flat-panel displays is manufactured using the slot-draw process[4] or the fusion process.[5] It is desirable to have glass manufactured with less surface warp and waviness, also referred to as better surface flatness, during these processes without altering its surface qualities. This paper presents the use of a hot pressurized gas, such as air or nitrogen, applied on both sides of a glass sheet to improve its flatness without surface contact.

2 Conventional surface-shaping methods

Several processes have been followed to change the surface topography of thin substrates. Double-sided polishing is commonly performed on thin silicon and glass wafers. This process is effective in reducing the total thickness variation of wafers, which are forced flat when inserted between the polishing pads; however, once removed from the tool, thin wafers tend to spring back to their inherent, wavy shape, a phenomenon commonly referred to as the potato-chip effect in the semiconductor industry.

Received 08/05/2009; accepted 12/19/2009.

The authors are with the Massachusetts Institute of Technology, 77 Massachusetts Ave., Rm. 37-487, Cambridge, MA 02139, USA; telephone 1+617-253-3180, e-mail: makilian@mit.edu and marks@space.mit.edu.

© Copyright 2010 Society for Information Display 1071-0922/10/1803-0240$1.00

A deterministic polishing process utilizing magneto-rheological fluids on thin sheets has been pursued by Heilmann *et al.*,[6] where 4-in.-diameter silicon wafers with an original surface warp of 2–3 μm peak-to-valley (*p–v*) were polished to <200 nm *p–v*. The results are promising; however, the low rate and high cost associated with this process make it feasible only when a few microns of surface material removal is sufficient, which is not the case of thin sheet glass. Furthermore, removing thin layers from the surface of sheet glass disturbs the residual compressive surface stresses that prevent crack propagation. Removing this surface layer can result in a new stress distribution with a different and possibly larger sheet warp. Polishing can potentially increase surface roughness, leave behind polishing contaminants, and introduce subsurface damage.

Perhaps the oldest method of shaping glass is the slumping process, wherein artisans heat glass until it is soft to change its shape. This art has been applied utilizing precision mandrels, where glass is heated to a temperature close to its softening point and then allowed to sag onto a thick, refractory mandrel with the desired surface shape, as shown in Fig. 1. In theory, by using a flat mandrel that has been accurately lapped and polished using conventional methods, the thin sheet of glass placed on the mandrel would sag as it is heated and replicate the mandrel's surface.[7–9] In practice, many challenges exist when slumping directly on a mandrel. Particulates such as dust and furnace-insulation debris present between the mandrel and the glass sheet introduce mid-to-high spatial-frequency errors on the surface of the sheet, as shown in Fig. 2. Such particles are difficult to completely eliminate between the two surfaces, even in a clean-room environment. The resulting mid-high spatial frequency errors are also difficult to correct in a subsequent step because it takes much longer periods of slumping time to remove such small dimples.

Stiction between the glass sheet and the mandrel is another difficult problem. Since slumping temperatures are typically high, ranging between 600 and 800°C, and the process of slumping relies on glass softening, it is very likely that the glass surface will fuse with the mandrel in the absence of a barrier between the two. If the mandrel is made of a thermally different material from the glass sheet,

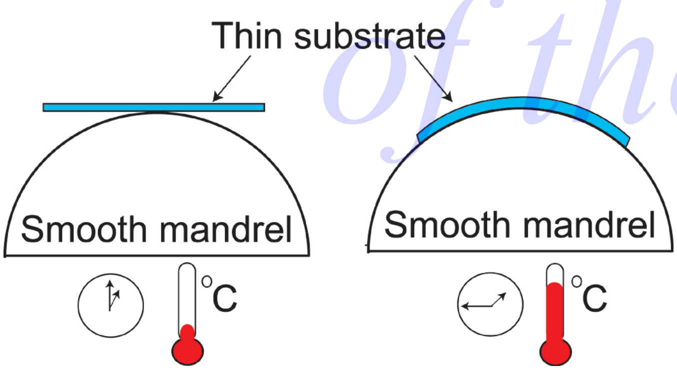

FIGURE 1 — A thin glass sheet slumped on a semi-cylindrical mandrel, replicating the surface of the mandrel.

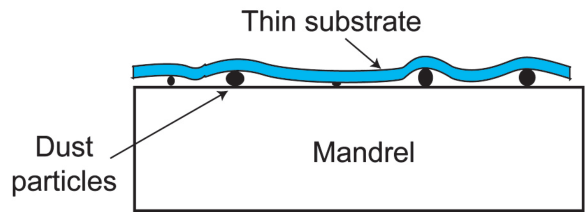

FIGURE 2 — Slumping of thin glass sheets on a mandrel with the presence of particulates between the two causing mid-high spatial-frequency dimples in the glass surface. Particle sizes are exaggerated for the purpose of illustration.

stiction can cause the sheet to crack during cooling as a result of the difference in the coefficients of thermal expansion (CTE) of the two materials, thus damaging both surfaces. In fact, particles serve as a barrier between the thin sheet and the mandrel but at the cost of imparting distortions into the glass sheet. Some attempts have been made to slump glass on a pin-chuck that provides discrete points of contact between the pins of the mandrel and the glass sheet[9,10]; however, fusion with the mandrel as the surface area of glass sheets increases remained a challenge. Slurry coatings, refractory cloths, and carbon and platinum coatings have been used in industry as non-stick surfaces between the glass sheet and the mandrel during slumping; however, the thickness uniformity of such intermediate layers must be tightly controlled to avoid introducing surface errors on the glass sheet, and they are only practical when working with individual sheets of glass slumped on a mandrel. Such a process cannot be applied to a continuous ribbon of glass, which is typically found in glass-sheet manufacturing plants.

3 Surface shaping utilizing pressurized gas and porous mandrels

The goal of this research is to reduce the flatness of glass sheet from its current state of hundreds of microns to a few microns *p–v*, without introducing high-spatial-frequency errors associated with entrapped particulates, and certainly without damaging the surface of the glass sheet due to fusion with mandrels. A contact-free method is demonstrated to achieve these requirements. This method utilizes a thin layer of gas, such as air or nitrogen, separating the glass sheet from the mandrel during slumping to avoid all the difficulties associated with contact during slumping.

Air bearings are utilized in many applications requiring high precision and very low friction, where a thin layer of pressurized air, typically 5–10 μm in thickness, separates the carried load from the bearing surface. This characteristic is useful when slumping glass sheets, where the pressurized air provides the slumping force while eliminating contact with the mandrel. For our experiments, we chose a gap of 50–100 μm, which is much larger than typical dust particles.

Air bearings come in many configurations.[11] Porous bearings have been chosen because they provide a continuous supply of pressurized gas along the bearing surface area.

Reprint from the Journal of the SID

The resulting force from the pressurized gas is needed to change the surface shape of the sheet as its temperature is increased to its softening point. Porous bearings, which will be referred to as mandrels from this point on, can be made with ceramics. This is an attractive feature because ceramics can be manufactured with high accuracy and can withstand the high temperatures required for slumping without creep.

The glass of interest in this set of experiments is Schott D-263, which is a borosilicate glass used in flat-screen displays. D-263 is manufactured using the down-draw process[12] and has a density of 2.51 g/cm^3, a Young's modulus of ~70 GPa at room temperature, and a softening point of 736°C. The substrate dimensions of interest for this research are 100 × 100 × 0.4 mm, providing a length-to-thickness ratio of 250. Although this particular glass was used in the experiments described in this paper, other types of sheet glass can be used as well to obtain similar results.

Glass sheets were placed between two porous mandrels, such that air flows through these mandrels and out against the glass surfaces, as shown in Fig. 3. The temperature of the experiment was raised from room temperature to 570°C, as shown in Fig. 4, at which point the D-263 glass was soft and responsive to the forces present in the thin gaps h_1 and h_2 on each side of the sheet. The experiment was held at this high temperature for a sufficient period of time for the glass sheet's surface topography to change, after which the temperature was slowly brought down to room temperature avoiding ceramic thermal shock, and the sheet

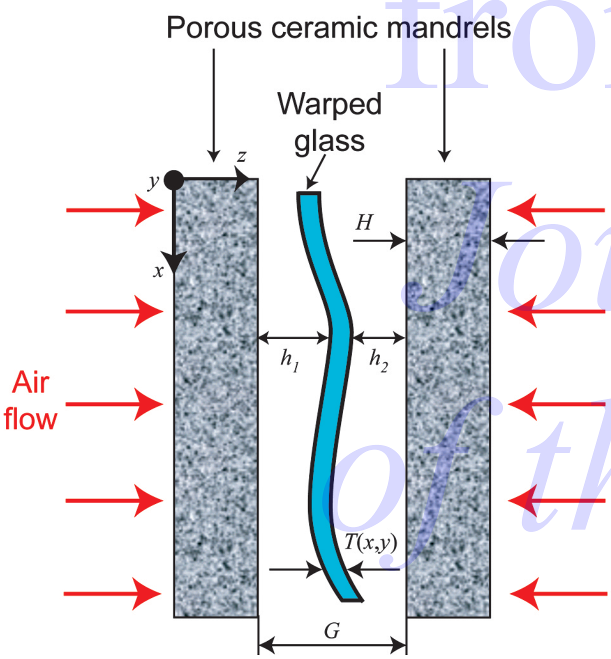

FIGURE 3 — A thin glass sheet placed between two porous, flat mandrels with air flowing through the mandrels and against the sheet to change its surface topography. The local pressure at any point along the length of the sheet varies with the size of the gap on each side. If h_1 is greater than h_2, the pressure at h_2 will push the glass sheet to the left until h_1 = h_2 (assuming equal supply pressures on both sides, equal pressure transmission through each mandrel and flat mandrels).

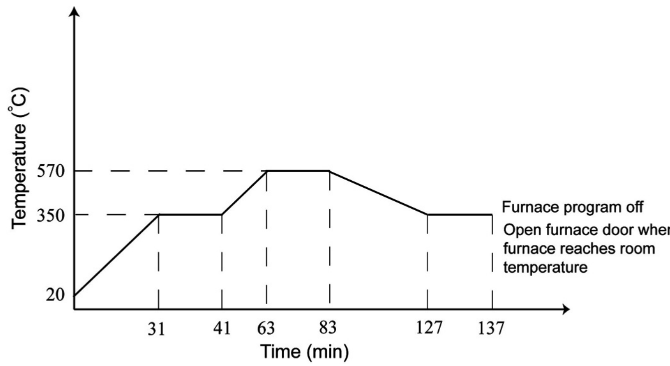

FIGURE 4 — A typical temperature cycle followed for slumping D-263 glass sheets between two porous mandrels.

was removed from between the two porous mandrels for evaluation.

Referring to the coordinate system shown in Fig. 3, the respective equations governing the flow through a porous mandrel and into the gap between the mandrel and the glass sheet are given below. These equations apply to the air flowing through the mandrel on one side of a glass sheet. Identical equations are applied to the mandrel on the other side of the sheet with different pressure and gap variables.

$$k_x \frac{\partial^2 p'}{\partial x^2} + k_y \frac{\partial^2 p'}{\partial y^2} + k_z \frac{\partial^2 p'}{\partial z^2} = 0, \tag{1}$$

$$\frac{\partial}{\partial x}\left[h\left(h^2 + 6k_x\right)\frac{\partial p}{\partial x}\right] + \frac{\partial}{\partial y}\left[h\left(h^2 + 6k_y\right)\frac{\partial p}{\partial y}\right] = 12k_z\left(\frac{\partial p'}{\partial z}\right)_{z=H}, \tag{2}$$

where $p(x,y)$ is the pressure in the gap of size $h(x,y)$ between the glass and the porous mandrel, $p'(x,y,z)$ is the pressure in the porous mandrel of thickness H, and k_x, k_y, and k_z are the permeability coefficients in the x, y, and z directions, respectively. These equations are derived from Darcy's equation of creeping flow in porous media with Reynold's number Re < 1, the continuity equation, and a modified Reynold's equation for flow between a porous and smooth surfaces. The detailed derivation of these equations can be found in Ref. 9.

The ceramic parts used were isotropic, thus the permeabilities k_x, k_y, and k_z were assumed equal and represented by k. To understand the effect of the size of the gap h and the resulting pressure distribution in the gap, Eq. (2) is simplified with the assumption that h is constant. It should be noted that k is on the order of 10^{-15} m^2, whereas h^2 is on the order of 10^{-12} m^2; thus $k << h^2$. In this case, Eq. (2) becomes

$$\frac{\partial^2 p}{\partial x^2} + \frac{\partial^2 p}{\partial y^2} = \frac{12k}{h^3}\left(\frac{\partial p'}{\partial z}\right)_{z=H}, \tag{3}$$

which shows that the distribution of pressure on the surface of the glass sheet at any given point is inversely proportional to the thickness cubed of the air gap h.

To better understand this phenomenon, Fig. 5 represents a simplified, one-dimensional situation with flow in

Reprint from the Journal of the SID

the x direction on each side of a heated glass sheet. A small step warp is introduced to the glass surface between two flat mandrels. The area of interest in Fig. 5 is 2Δ long. For this one-dimensional flow scenario, Eq. (3) governing the flow in the gap on each side of the glass sheet reduces to

$$\frac{d^2p}{dx^2} = \frac{12k}{h^3}\left(\frac{\partial p'}{\partial z}\right)_{z=H}, \tag{4}$$

which when integrated twice with respect to x results in a parabolic distribution of pressure of the form

$$p = \frac{12k}{h^3}\left(\frac{\partial p'}{\partial z}\right)_{z=H} x^2 + Bx + C \tag{5}$$

on each side of the sheet, where B and C are coefficients depending on the boundary conditions of the area 2Δ. In order to isolate the effect of the gap, we assume that the boundary conditions are identical on both sides of the sheet, with constant gap $\hat{h}$, so that coefficients B and C are also the same on both sides. In this case, the right side of the sheet in Fig. 5, where the gap h_2 is smaller, would have a higher first coefficient than the left side of initial gap $h_1 > h_2$. Thus, the resulting higher pressure on the right side of the sheet acting along the length 2Δ pushes the sheet towards the left until equilibrium of forces is obtained, which happens when $h_1 = h_2 = \hat{h}$ for equal flow supply pressures.

Looking at the entire warped sheet in Fig. 3, the gap at any point along the length of the glass will be larger on one side than the other, as demonstrated in the figure, where $h_1 > h_2$ at one point. The glass sheet thickness is represented by $T(x,y)$. The predefined distance between the two porous, flat mandrels is represented by G. For equal supply pressures and mandrel permeabilities, the local pressure at h_2 will be larger than the local pressure at the equivalent point h_1 on the other side of the sheet. As the glass softens with temperature, this difference in local pressure pushes that part of the sheet until the pressures on both sides are equal, such that $h_1(x,y) = h_2(x,y) = \hat{h}(x,y)$, where $\hat{h}(x,y) = [G - T(x,y)]/2$. Thus, the entire surface area of an initially warped glass sheet placed between two flat mandrels is shaped by the local pressures, and the surface waviness can be dramatically reduced from the original hundreds of microns to a few microns. In order to remove the effects of the weight of the glass sheet during slumping, this process was conducted in the vertical plane.

Individual sheets were used to demonstrate the concept of reducing the surface warp of sheet glass using pressurized air through porous mandrels at elevated temperatures; however, the same concept can be applied on continuous ribbons of glass, where larger porous mandrels can be used such that the ribbon passes between the two mandrels, as shown in Fig. 6. A tapered top can facilitate inserting a warped glass sheet in the gap between the two flat, porous mandrels.

Reprint from the Journal of the SID

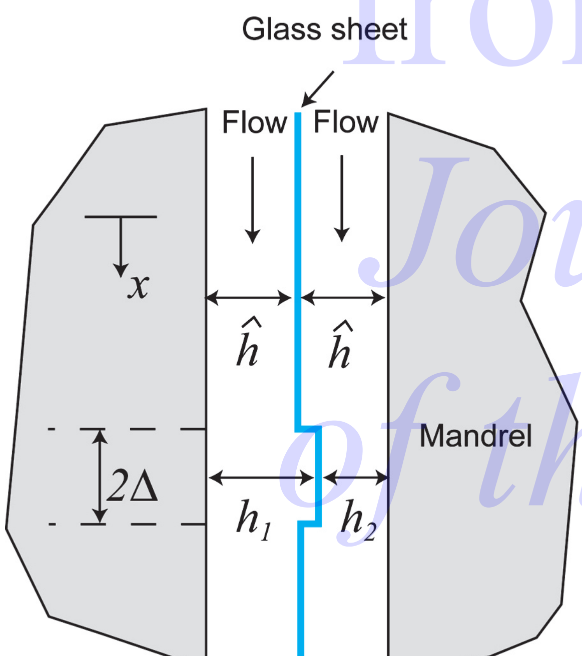

FIGURE 5 — A simplified, one-dimensional flow against the two surfaces of a heated glass sheet with a step warp. Gap h_1 is larger than h_2 along the length 2Δ; thus, the pressure on the left side is lower than the equivalent pressure on the right side, and the glass sheet is pushed to the left until equilibrium is established, reducing the warp of the glass.

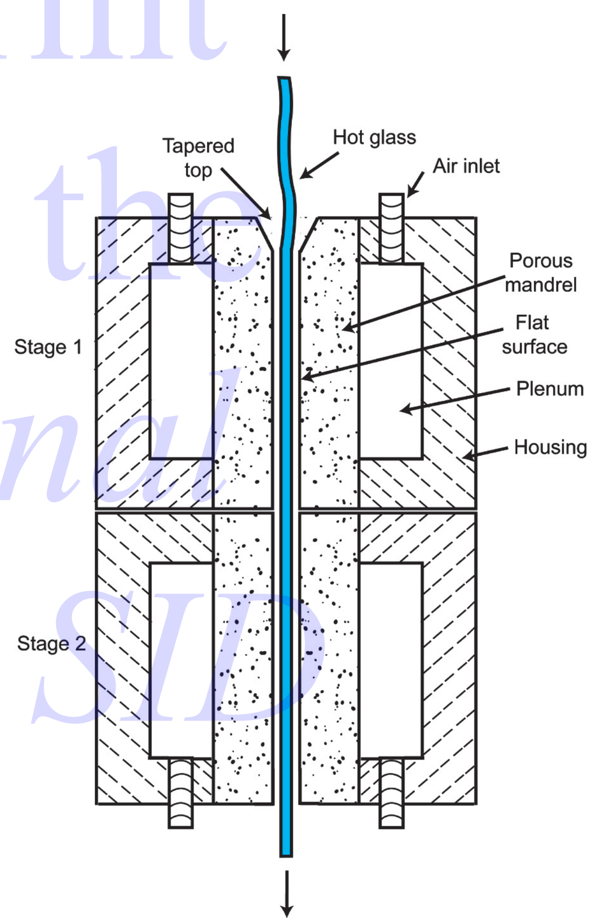

FIGURE 6 — Depiction of a continuous glass ribbon passing between flat porous mandrels to reduce its surface warp. The two stages represent slumping performed at different temperatures with the temperature in Stage 1 being higher than that of Stage 2.

It should be noted that this process only works when the glass is in a fluid state; thus, slumping must be performed above the glass-transformation temperature, which is the point where the viscosity of the glass sheet changes such that it transforms from a solid to a fluid state. In fact, the higher the temperature of the sheet, the quicker its response to gas forces, since the relaxation time for glass decreases as its temperature increases. Thus, depending on the velocity of the sheet flowing downwards, the ideal temperature for slumping can be calculated such that the sheet has enough time to deform with the gas forces as it travels along the length of the mandrels.

As the hot glass ribbon flows continuously downwards during manufacturing, its temperature must be reduced for it to solidify; therefore, if the glass is passing between pairs of mandrels, the gas going through the mandrels must be at a controlled temperature along the length of the sheet. Although glass solidifies once its temperature goes below the transformation point, it is recommended to continue with the slumping between two mandrels at temperatures below the transformation point to ensure that the glass has completely solidified and any forces from vibration and temperature gradients would no longer imprint on the sheet. This can be done by having different sections, as shown in Fig. 6, where the temperature in the sections decreases along the length of the sheet as it flows downwards.

4 Design of apparatus

When designing the apparatus for slumping glass between two porous mandrels, several factors must be taken into account, such as thermal stresses and strains and their effect on the final shape of the glass sheet, the distance between the glass sheet and the mandrels on each side and the pressure distribution in the gap between the glass sheet and each of the mandrels.

Silicon carbide mandrels with 40% porosity were purchased from Refractron. Silicon carbide offers exceptional mechanical and thermal properties. Dry grinding was performed by Professional Instruments on the top surface of these mandrels to obtain a surface topography of about 1-μm *p–v* for one and 3-μm *p–v* for the other in the central area of each. The edges were found to be more warped as a result of the grinding process.

A housing structure is required in order to provide a plenum with a constant supply pressure on the back side of the mandrel, as shown in Fig. 6. The housing must withstand the high slumping temperatures without inducing any thermal stresses and strains on the flat mandrel. Porous silicon carbide was chosen for the housing as well. In fact, one large silicon carbide plate was purchased, 12 × 12 × 0.5 in. in dimensions and was divided into four plates to form two mandrels and two housing structures, each having overall dimensions of 6 × 6 × 0.5 in. This ensures similar permeabilities for both mandrels, which results in less pressure variations across the thickness of each mandrel as a result of permeability variation. Because the housing is porous, air leakage through the housing could have been a concern, in which case a glassy glaze could have been used to seal the housing and the side walls of the mandrel; however, the very small leakage through the porous walls did not render itself problematic.

Ideally, a mechanical means would be used to set the gap between the mandrels, such that the plates and/or the glass ribbon may move unimpeded. In order to simplify our experiments, small tantalum spacers manufactured by A. D. Mackay were placed at the four corners between the mandrels to set the gap h between the glass sheet and each of the two mandrels at 50 μm in this set of experiments. This facilitates inserting thin glass sheets that have an original surface waviness of hundreds of microns between the two flat mandrels. This gap is rather large compared to what is typically recommended for air-bearing applications; however, viscous flow is still achieved in the case of slumping at elevated temperatures close to 600°C because the viscosity of air is over twice its value at room temperature and the flow velocity is very small.[9] It should also be noted that the flow of air in this case is used to shape the soft, hot glass and not to carry heavy loads typically borne by air bearings.

With the current design, two pairs of mandrels and housings were used to slump glass, each pair placed on one side of the glass. The overall assembly was clamped together using stainless-steel plates and a set of rods and nuts, as shown in Fig. 7. The resulting compressive force is imposed on the center of the ceramic plates, while leaving their

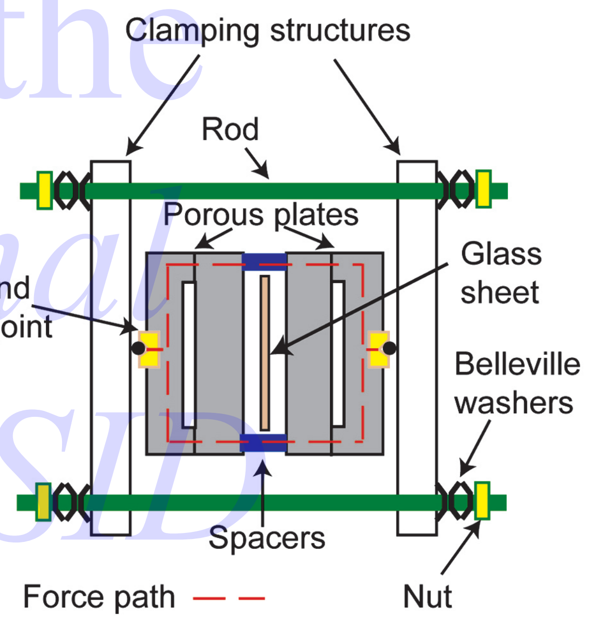

FIGURE 7 — The assembly of the porous ceramic plates using metal support plates and rods, nuts, and belleville washers. The figure is not to scale. The clamping structures connect at the center of the ceramic plates to allow the ceramic edges to expand freely as the temperature is raised. Spacers at the corners of the mandrels were only used in this prototype to set the gap and would not be used in actual manufacturing processes. The path of the compressive force resulting from clamping traverses the porous plates and spacers and does not go through the glass sheet.

Reprint from the Journal of the SID

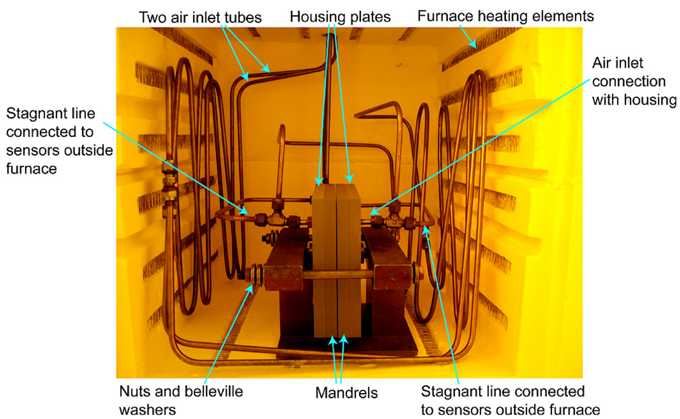

FIGURE 8 — Photograph of a sheet of glass (not seen in image) held between two flat mandrels ready for slumping inside a furnace of dimensions 11-in. wide × 15-in. high × 13-in. deep.

edges free, allowing the ceramic to expand at a different rate from the metal plates without distortion. The interface between the stainless-steel plate and the ceramic housing is a ball and cone joint, as shown in Fig. 7. It should be noted that the clamping compressive force applied at the center of each of the housing ceramic plates traverses from one side to the other through the mandrel and spacers; however, this force does not go through the glass sheet slumped, as illustrated in Fig. 7.

Figure 8 shows the assembled ceramic plates inside a furnace. A glass sheet, not visible in the picture, is constrained between the two porous mandrels. Two independent pressure lines were introduced into the furnace in the form of 4-m-long bent tubes and connected to each housing. The long tubes ensure the air is heated to the required slumping temperature before going through the porous mandrels and shaping the glass. The two tubes were bent identically and placed close to each other inside the furnace to ensure both were heated at the same rate and to avoid resulting pressure fluctuations in the lines. It should also be noted that a stagnant line was taken from each plenum to the outside, where it was connected to high-precision-pressure transducers monitoring the pressure inside each plenum throughout the experiment. A schematic diagram shown in Fig. 9 demonstrates this layout.

Having controlled pressure on each side of the glass sheet is very critical. Because the assembled parts were placed in a high-temperature environment during testing, pressure gauges and flow-control valves were placed outside the furnace, thereby controlling the flow characteristics outside the furnace, where the air is at room temperature. At the beginning of every experiment, the air flowing into the two plenums was adjusted such that the pressure in one stagnant line connected to one plenum was equal to the other. This pressure was then monitored throughout the experiment and the flow further adjusted as necessary to ensure equal pressure in both plenums. The starting pressure at room temperature was close to 0.06 psi in each plenum, which increased to about 0.25 psi at a constant flow rate as the temperature was raised. This low working pressure was sufficient to reduce the inherent warp of 0.4-mm-thick glass.

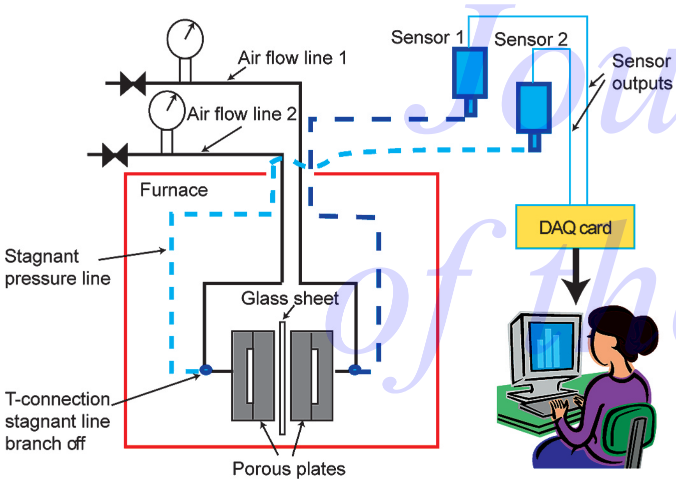

FIGURE 9 — A T-connection is used before the plenum to divide the incoming pressure line into a stagnant one, connected to sensors outside the furnace environment, and a dynamic one going into the plenum to shape glass. The sensor output is connected to a National Instruments Data Acquisition Card (DAQ Card), which in turn connects to a computer to plot the pressure variation with time as the experiment proceeds.

5 Results and discussion

Several sheets of glass with dimensions of 100 × 100 × 0.4 mm have been slumped using the pressurized air method. Surface metrology was conducted using a Shack–Hartmann system, which has a repeatability of 40-nm *p–v*,[13] while the glass was constrained using a specially designed metrology truss that constrains thin optics with a repeatability of 50-nm *p–v*.[14]

Sheet glass is typically manufactured in the form of continuous ribbons flowing vertically downward, as was described in Sec. 1; however, this is difficult to replicate

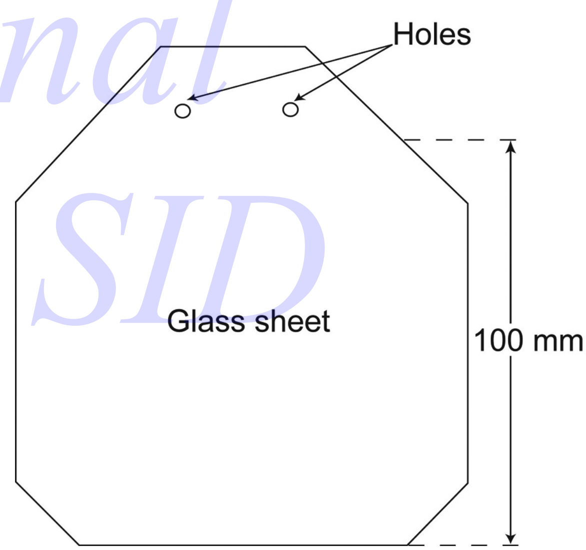

FIGURE 10 — Two holes, 1/16 in. in diameter, are machined in glass sheets using laser ablation. The glass sheet is suspended by wires between the two porous mandrels during the shaping process.

Reprint from the Journal of the SID

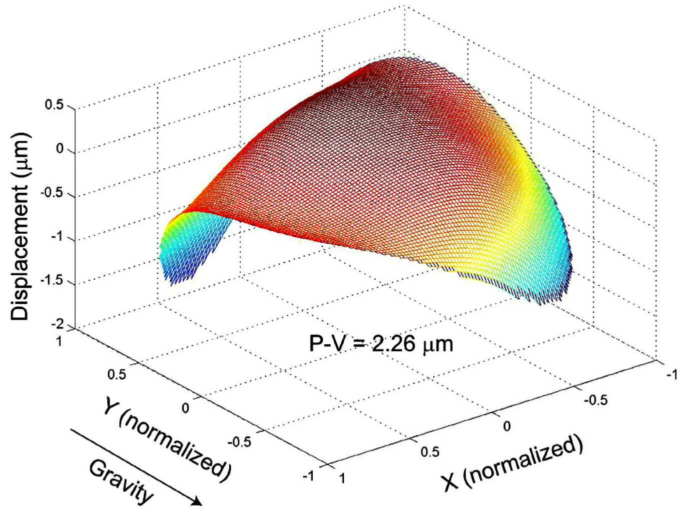

FIGURE 11 — Measured surface of a glass sheet after slumping while being suspended by wires resulting in a 2.26-µm *p–v* warp. The aperture is 60 mm. The gravity vector is aligned with the *y* axis.

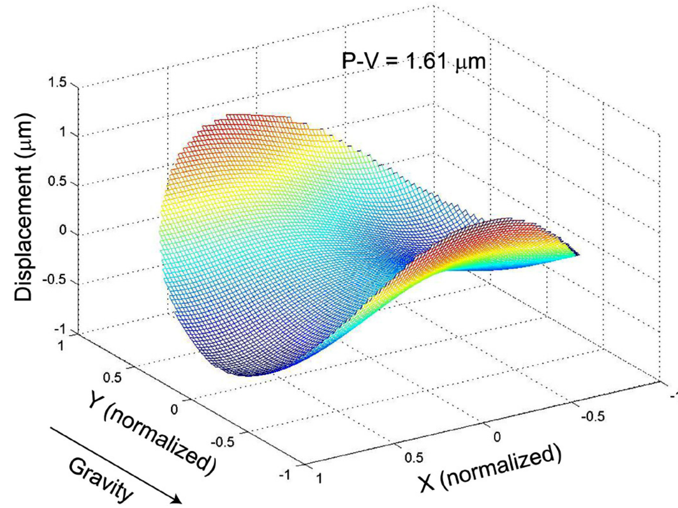

FIGURE 13 — Measured difference of the surfaces of two glass sheets slumped while being suspended by wires resulting in a 1.61-µm *p–v* warp. The aperture is 60 mm. The gravity vector is aligned with the *y* axis.

inside a confined furnace space in a laboratory environment. Thus, glass sheets were suspended between the two mandrels while they were shaped by the pressurized gas. This was accomplished by machining two holes 1/16 in. in diameter on sheets using laser ablation, as shown in Fig. 10. The holes were located outside the working area of 100 × 100 mm, and thin metal wires through the holes were used to hang the glass sheets between the two porous mandrels.

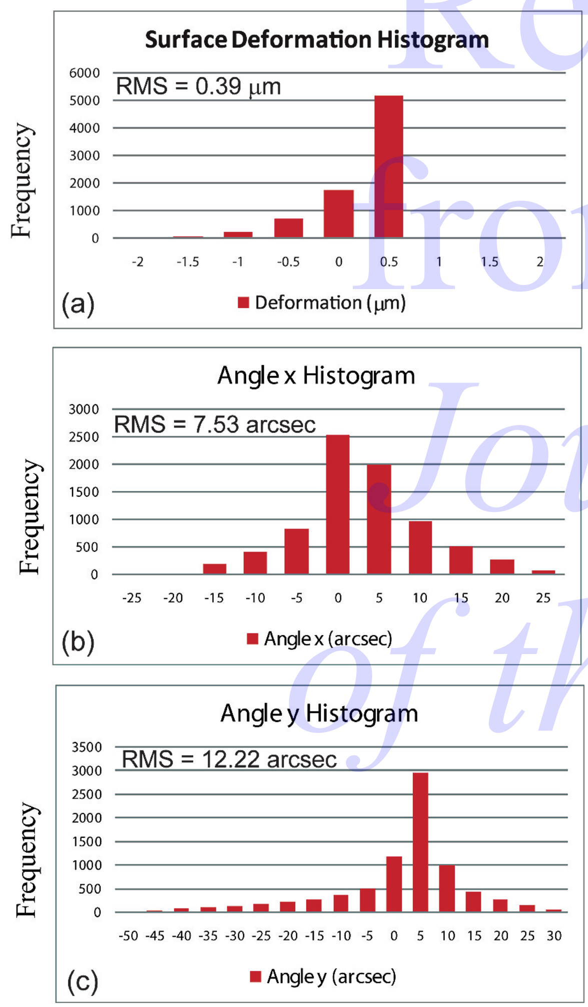

FIGURE 12 — Histograms of the glass sheet shown in Fig. 11.

Figure 11 shows the result from a sheet after it had been slumped while being suspended by wires. The initial warp of sheets with such geometry varies between 80- and 600-µm *p–v*. As can be seen, the overall surface after shaping with the pressurized gas method has a topography of 2.3-µm *p–v* and 0.39-µm rms. Histograms are also included in Fig. 12 to better understand the distribution of the data, where a large percentage of the surface area is between –0.5 and 0.5 µm.

To understand how the process repeats, sheets obtained from different slumping tests were compared, and the result is shown in Fig. 13. The overall surface difference between runs varies by 1.6-µm *p–v* and 0.35-µm rms. Histograms are shown in Fig. 14.

A major source of process repeatability error is the inability to precisely control the pressures in each plenum such that they are identical during every run. This is because the tool's flow control valves have a coarse resolution, making it difficult for the user to open them the exact same amount every time an experiment is conducted. An easy solution is to replace these valves with high-precision-flow controllers that can connect to the pressure transducers reading the pressure inside each plenum to form a closed-loop system.

Other sources of error in the repeatability of the process include the thickness variation of different glass sheets and the exact alignment angle of the ceramic mandrel surfaces with gravity. The latter is believed to cause the larger surface warp seen in the *y* direction of the sheets, which is aligned with the gravity vector. All these aspects will be addressed in the near future to improve both the accuracy and the repeatability of the current setup.

Reprint from the Journal of the SID

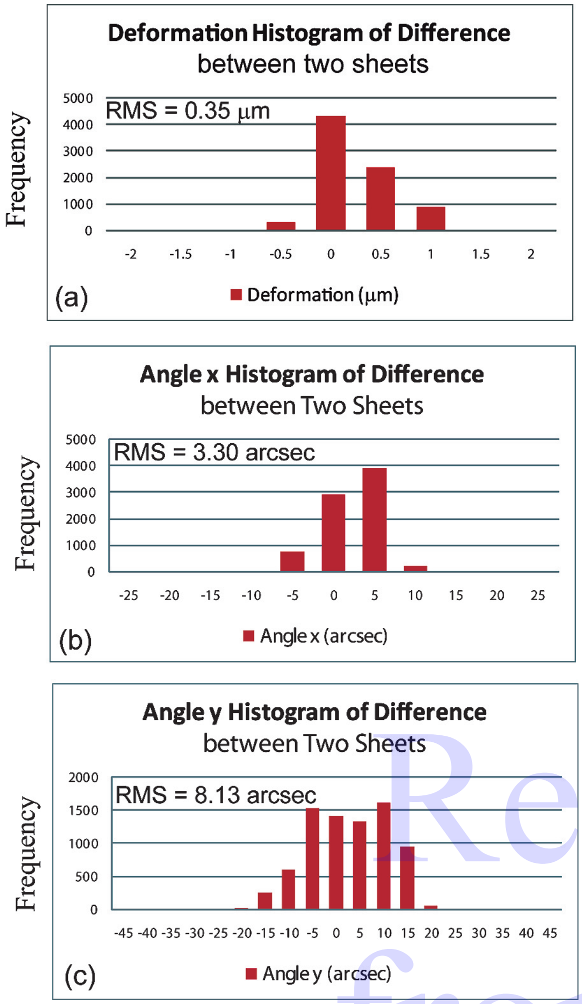

FIGURE 14 — Histograms of the difference data shown in Fig. 13.

A big advantage of this process is the absence of the effects of entrapped particulates on the surface of slumped glass sheets. The process requires minimal cleaning using a quick air blast before every run, yet surface dimples from particulates were absent. The glass sheet maintains its pristine optical qualities after slumping, which is highly desired in the flat-panel display and high precision optics industries. With larger heating elements and porous mandrels, larger sizes of glass sheets can be shaped to reduce their warp and waviness, where the glass can be in the form of individual sheets or continuous ribbons.

6 Conclusion

A new process was developed utilizing two flat, porous mandrels placed parallel to each other at a predetermined distance, with 0.4-mm-thick sheet glass suspended between the two mandrels. Pressurized gas flowing through these mandrels and against the glass sheet was used to change the surface topography of the sheet. The process was conducted at elevated temperatures close to the softening temperature of the glass used. The resulting surface warp of the sheets was reduced from hundreds of microns to a couple of microns. Because no physical contact occurs with the glass sheets during this process, the resulting optical surface qualities are unchanged.

Acknowledgments

We wish to thank the students and staff from the Space Nanotechnology Laboratory for their support. The efforts of the staff of the MIT Central and Kavli machine shops are highly appreciated. This work is supported by NASA Grants NNG05WC14G and NAG5-12583.

References

1 Business Wire. "Strategy Analytics Projects 66 Percent Flat Panel TV Revenue Increase in 2005; 17.5 Million Unit Sales Generates $25 Billion" (2005).
2 R. H. Mauch *et al.*, "Thin glass substrates for mobile applications," *Proc. SPIE, Inorganic Optical Materials II* **4102**, 162–168 (2000).
3 J. C. Lapp *et al.*, "Advanced glass substrates for flat panel displays," *Proc. SPIE, Advanced Flat Panel Display Technologies* **2174**, 129–138 (1994).
4 W. C. Hynd, "Flat glass manufacturing processes," *Glass Science Technol.* **2**, 83–100 (1984).
5 S. M. Dockerty, *Sheet Forming Apparatus,* U.S. Patent 3,338,696 (1967).
6 R. K. Heilmann *et al.*, "Shaping of thin grazing-incidence reflection grating substrates via magnetorheological finishing," *Proc. SPIE, Optics for EUV, X-Ray, and Gamma-Ray Astronomy II* **5900**, 73–80 (2005).
7 M. Jimenez-Garate, *The Development of Hard X-ray Telescope Optics and a Theoretical Model of X-ray Emission from Accretion Disks,* Ph.D. Thesis (Columbia University, Graduate School of Arts and Sciences, 2001).
8 R. Petre *et al.*, "The Constellation-X spectroscopy X-ray telescope: Recent technology development," *Proc. SPIE, Space Telescopes and Instrumentation II: UV to Gamma Ray* **6266**, 62661Q (2006).
9 M. Akilian, *Methods of Improving the Surface Flatness of Thin Glass Sheets and Silicon Wafers,* Ph.D. Thesis (Massachusetts Institute of Technology, Department of Mechanical Engineering, 2008).
10 R. Heilmann *et al.*, "Novel methods for shaping thin-foil optics for x-ray astronomy," *Proc. SPIE, X-Ray Optics for Astronomy: Telescopes, Multilayers, Spectrometers, and Missions* **4496**, 62–72 (2001).
11 A. H. Slocum, *Precision Machine Design* (Society of Manufacturing Engineers, 1992), pp. 580–589.
12 Schott North America, *D 263 Thin Glass,* 555 Taxter Rd, Elmsford, N.Y.
13 C. R. Forest *et al.*, "Metrology of thin transparent optics using Shack–Hartmann wavefront sensing," *Opt. Eng.* **43**, 742–753 (2003).
14 M. Akilian *et al.*, "Thin optic constraint," *Precision Eng.* **31**, 130–138 (2007).

Mireille Akilian is an Associate at Exponent in Natick, MA. Her principal interests include precision engineering, mechanical system design, and testing and failure. She received her B.E. degree from the American University of Beirut (mechanical engineering, 2002), M.S. degree from the Massachusetts Institute of Technology (mechanical engineering, 2004), and a Ph.D. degree from the Massachusetts Institute of Technology (mechanical engineering, 2008). She is a member of SPIE and the American Society for Precision Engineering.

Reprint from the Journal of the SID

Mark L. Schattenburg is Senior Research Scientist at the MIT Kavli Institute of Astrophysics and Space Research and Director of the Space Nanotechnology Laboratory. His principal interests include micro/nanofabrication technology, optical and x-ray interferometry, x-ray optics and telescope technology, and high-precision optics fabrication and assembly. He has been involved with the fabrication of precision diffraction gratings spectrometers for numerous NASA missions, including the *Chandra* x-ray telescope, and is a member of several NASA mission technology development teams. He received his B.S. degree from the University of Hawaii (physics, 1978) and Ph.D. from MIT (physics, 1984). He was appointed Postdoctoral Associate at MIT in 1984, progressing to Senior Research Scientist in 2004. He has published over 160 papers and holds six patents. He is a member of the Optical Society of America, the American Vacuum Society, SPIE, the IEEE, and the American Society for Precision Engineering.

Reprint from the *Journal of the SID*